

RESEARCH ARTICLE | AUGUST 22 2004

## Calculation of exchange-correlation potentials with auxiliary function densities

Andreas M. Köster; J. Ulises Reveles; Jorge M. del Campo



*J. Chem. Phys.* 121, 3417–3424 (2004)

<https://doi.org/10.1063/1.1771638>



### Articles You May Be Interested In

Hermite Gaussian auxiliary functions for the variational fitting of the Coulomb potential in density functional methods

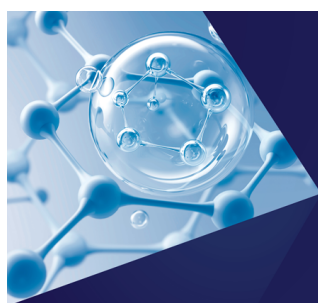
*J. Chem. Phys.* (June 2003)

Auxiliary density perturbation theory

*J. Chem. Phys.* (April 2008)

Density-functional expansion methods: Generalization of the auxiliary basis

*J. Chem. Phys.* (May 2011)



The Journal of Chemical Physics  
**Special Topics Open  
for Submissions**

[Learn More](#)

# Calculation of exchange-correlation potentials with auxiliary function densities

Andreas M. Köster, J. Ulises Reveles, and Jorge M. del Campo

*Departamento de Química, CINVESTAV, Avenida Instituto Politécnico Nacional 2508, Apartado Postal 14-740, Mexico D.F. 07000, Mexico*

(Received 21 April 2004; accepted 19 May 2004)

The use of Hermite Gaussian auxiliary function densities from the variational fitting of the Coulomb potential for the calculation of exchange-correlation potentials is discussed. The basic working equations for the energy and gradient calculation are derived. The accuracy of this approximation for optimized structure parameters and bond energies are analyzed. It is shown that the quality of the approximation can be systematically improved by enlarging the auxiliary function set. Average errors of 0.5 kcal/mol are obtained with auxiliary function sets including  $f$  and  $g$  functions. The timings for a series of alkenes demonstrate a substantial performance improvement. © 2004 American Institute of Physics. [DOI: 10.1063/1.1771638]

## I. INTRODUCTION

The development of efficient algorithms for the calculation of electron repulsion integrals<sup>1–5</sup> has considerably improved the performance of quantum chemistry methods. This is particularly true for density functional theory (DFT) methods using the variational approximation of the Coulomb potential.<sup>6–10</sup> In these methods only three-center electron repulsion integrals are needed. Recently, very efficient integral algorithms for these three-center electron repulsion integrals have been developed.<sup>11</sup> With these algorithms a near linear scaling for the calculation of the three-center Coulomb integrals can be achieved.<sup>12</sup> As a consequence the numerical integration of the exchange-correlation potential becomes the most time demanding step in the construction of the Kohn-Sham matrix.

The use of auxiliary functions for the calculation of the exchange-correlation potential has a long history in DFT methods.<sup>13,14</sup> In programs like DEMON-KS,<sup>15</sup> DGAUSS,<sup>16</sup> or GTOFF (Ref. 17) the exchange-correlation potential is expanded in auxiliary functions as proposed by Sambe and Felton.<sup>14</sup> The expansion coefficients are obtained by a least square fit on a grid. Because this fit is not variationally only approximated gradients are available. This can introduce noise in the geometry optimization and in higher energy derivatives.

As an alternative to this approach the direct use of the auxiliary function density from the variational fitting of the Coulomb potential for the calculation of the exchange-correlation potential has been investigated over the last years.<sup>18,19</sup> If the auxiliary function density is used for the evaluation of the exchange-correlation potential it is desirable that it is positive definite and integrates to the number of electrons in the system. Whereas, the normalization to the number of electrons can be easily included into the variational fitting of the Coulomb potential the positive definiteness of the approximated density is not guaranteed. However, the construction of the approximated density by itself avoids the accumulation of larger areas with negative

densities.<sup>20</sup> As soon as a region accumulates negative fitted density it acts as an attractive potential for the remaining electron density. Because the fitting is variational in the Coulombic self-energy error negative fitted density regions almost never occur. In fact, in the numerical integration of the approximated density, grid points with negative density values are simply screened without sacrificing the accuracy of the numerically integrated electron number. The errors in the electron count introduced by this screening procedure are typically in the range of  $10^{-5}$  and, therefore, within the usually used grid accuracy for the numerical integration.

Because the approximated density is a linear combination of auxiliary functions the density calculation at each grid point becomes linear. Instead, with the orbital density products of basis functions have to be evaluated. Obviously, this represents a considerable simplification of the grid work. However, the number of auxiliary functions is usually three to five times the number of basis functions. This could deteriorate the performance of the approximated density calculation on the grid because the calculation of the exponential function is computationally not negligible. Therefore, we are using in our implementation primitive Hermite Gaussian functions which are grouped together in sets, sharing the same exponents. As an example, a  $d$  auxiliary function set contains ten primitive Hermite Gaussians, one  $s$ , three  $p$ , and six  $d$  functions, all with the same exponent. Thus, the number of exponents that have to be evaluated at each grid point is for an auxiliary function density of this structure much smaller than for the corresponding orbital density. Moreover, by using Hermite Gaussian auxiliary functions the Hermite polynomial recurrence relations<sup>21</sup> can be used for the function calculation on the grid.

In this paper we develop the basic working equations for the use of the auxiliary function density from the variational fitting of the Coulomb potential for the calculation of the exchange-correlation potential. To avoid unnecessary complications in the presentation we restrict ourselves to the closed-shell case with a local functional. In the following section the self-consistent field (SCF) energy calculation will

be described. In Sec. III, the corresponding energy gradients are derived. The computational methodology is given in Sec. IV. The validation and performance of the calculation of the exchange-correlation potential with the auxiliary function density are discussed in Sec. V. Concluding remarks are drawn in the last section. The algorithms presented in this paper are implemented in the DFT code deMon.<sup>22</sup>

## II. SCF ENERGY

The variational approximation of the Coulomb potential, as implemented in deMon, is based on the minimization of the following self-energy error:

$$\mathcal{E}_2 = \frac{1}{2} \int \int \frac{[\rho(\mathbf{r}_1) - \tilde{\rho}(\mathbf{r}_1)][\rho(\mathbf{r}_2) - \tilde{\rho}(\mathbf{r}_2)]}{|\mathbf{r}_1 - \mathbf{r}_2|} d\mathbf{r}_1 d\mathbf{r}_2. \quad (1)$$

In the linear combination of Gaussian type orbital (LCGTO) approximation, the orbital density  $\rho(\mathbf{r})$  is given as

$$\rho(\mathbf{r}) = \sum_{\mu, \nu} P_{\mu\nu} \mu(\mathbf{r}) \nu(\mathbf{r}). \quad (2)$$

Here  $\mu(\mathbf{r})$  and  $\nu(\mathbf{r})$  represent contracted atomic Gaussian orbitals and  $P_{\mu\nu}$  is an element of the (closed-shell) density matrix that is defined over the molecular orbital coefficients  $c_{\mu i}$  as

$$P_{\mu\nu} = 2 \sum_i^{\text{occ}} c_{\mu i} c_{\nu i}. \quad (3)$$

The approximated density  $\tilde{\rho}(\mathbf{r})$  is expanded in primitive Hermite Gaussians  $\bar{k}(\mathbf{r})$  which are centered at the atoms:

$$\tilde{\rho}(\mathbf{r}) = \sum_{\bar{k}} x_{\bar{k}} \bar{k}(\mathbf{r}). \quad (4)$$

The primitive Hermite Gaussian function, from now on indicated by a bar, at atom  $K$  with the exponent  $\zeta_k$  has the form:

$$\begin{aligned} \bar{k}(\mathbf{r}) &= \left( \frac{\partial}{\partial K_x} \right)^{\bar{k}_x} \left( \frac{\partial}{\partial K_y} \right)^{\bar{k}_y} \left( \frac{\partial}{\partial K_z} \right)^{\bar{k}_z} e^{-\zeta_k(\mathbf{r}-\mathbf{K})^2} \\ &= \lambda_{\bar{k}_x}(x_K) \lambda_{\bar{k}_y}(y_K) \lambda_{\bar{k}_z}(z_K) e^{-\zeta_k(\mathbf{r}-\mathbf{K})^2}, \end{aligned} \quad (5)$$

with

$$\lambda_{\bar{k}_x}(x_K) = \zeta_k^{\bar{k}_x/2} H_{\bar{k}_x}(\zeta_k^{1/2} x_K). \quad (6)$$

$H_{\bar{k}_x}$  denotes a Hermite polynomial of the order  $\bar{k}_x$ . As already mentioned the exponential part is shared by all functions of an auxiliary function set and, therefore, has only to be calculated one time at each grid point. For the polynomials  $\lambda_{\bar{k}_x}$ ,  $\lambda_{\bar{k}_y}$ , and  $\lambda_{\bar{k}_z}$ , the following recurrence relation can be deduced:

$$\lambda_{\bar{k}_x+1}(x_K) = \lambda_{\bar{k}_x}(x_K) \lambda_{\bar{k}_x}(x_K) - 2\zeta_k \bar{k}_x \lambda_{\bar{k}_x-1}(x_K), \quad (7)$$

with

$$\lambda_{\bar{0}}(x_K) = 1, \quad (8)$$

$$\lambda_{\bar{1}}(x_K) = 2\zeta_k x_K. \quad (9)$$

Therefore, only  $\lambda_{\bar{0}}$  and  $\lambda_{\bar{1}}$  have to be initialized and all higher polynomials can be generated by Eq. (7). The function argument  $x_K$  represents the difference between the grid point and the atomic  $x$  coordinate in the above formulation.

With the Hermite Gaussian auxiliary function density the following SCF energy expression is obtained:

$$\begin{aligned} E_{SCF} &= \sum_{\mu, \nu} P_{\mu\nu} H_{\mu\nu} + \sum_{\mu, \nu} \sum_{\bar{k}} P_{\mu\nu} \langle \mu \nu \| \bar{k} \rangle x_{\bar{k}} \\ &\quad - \frac{1}{2} \sum_{\bar{k}, \bar{l}} x_{\bar{k}} x_{\bar{l}} \langle \bar{k} \| \bar{l} \rangle + E_{xc}[\tilde{\rho}]. \end{aligned} \quad (10)$$

In this notation the symbol  $\|$  stands for the Coulomb operator  $1/|\mathbf{r}_1 - \mathbf{r}_2|$ . The difference to the usual energy expression of the variational fitting of the Coulomb potential<sup>23</sup> is the appearance of the fitted density in the exchange-correlation energy term.

The expansion coefficients  $x_{\bar{k}}$  of the approximated density are calculated by the minimization of the self-energy error  $\mathcal{E}_2$ :

$$\frac{\partial \mathcal{E}_2}{\partial x_m} = - \sum_{\mu, \nu} P_{\mu\nu} \langle \mu \nu \| \bar{m} \rangle + \sum_{\bar{k}} x_{\bar{k}} \langle \bar{k} \| \bar{m} \rangle = 0 \quad \forall \bar{m}. \quad (11)$$

To ensure the normalization of the approximated density to the electron number the following constraint is applied:

$$\int \tilde{\rho}(\mathbf{r}) d\mathbf{r} = \sum_{\bar{k}} x_{\bar{k}} \langle \bar{k} \rangle = N, \quad \text{with} \quad \langle \bar{k} \rangle = \int \bar{k}(\mathbf{r}) d\mathbf{r}. \quad (12)$$

Here  $N$  denotes the number of the electrons in the system calculated as

$$N = \sum_{\mu, \nu} P_{\mu\nu} S_{\mu\nu}. \quad (13)$$

Using Eqs. (11) and (12) the following equation system for the determination of the expansion coefficients of the approximated density is obtained:

$$\begin{pmatrix} \mathbf{J} \\ N \end{pmatrix} = \mathbf{G} \begin{pmatrix} \mathbf{x} \\ \lambda \end{pmatrix} \Rightarrow \begin{pmatrix} \mathbf{x} \\ \lambda \end{pmatrix} = \mathbf{G}^{-1} \begin{pmatrix} \mathbf{J} \\ N \end{pmatrix} \quad (14)$$

with

$$\mathbf{J} = \begin{pmatrix} \sum_{\mu, \nu} P_{\mu\nu} \langle \mu \nu \| \bar{1} \rangle \\ \sum_{\mu, \nu} P_{\mu\nu} \langle \mu \nu \| \bar{2} \rangle \\ \vdots \\ \sum_{\mu, \nu} P_{\mu\nu} \langle \mu \nu \| \bar{m} \rangle \end{pmatrix}, \quad \mathbf{x} = \begin{pmatrix} x_{\bar{1}} \\ x_{\bar{2}} \\ \vdots \\ x_{\bar{m}} \end{pmatrix}, \quad (15)$$

and

$$\mathbf{G} = \begin{pmatrix} \langle \bar{1} | \bar{1} \rangle & \langle \bar{1} | \bar{2} \rangle & \dots & \langle \bar{1} | \bar{m} \rangle & \langle \bar{1} | \\ \langle \bar{2} | \bar{1} \rangle & \langle \bar{2} | \bar{2} \rangle & \dots & \langle \bar{2} | \bar{m} \rangle & \langle \bar{2} | \\ \vdots & \vdots & \ddots & \vdots & \vdots \\ \langle \bar{m} | \bar{1} \rangle & \langle \bar{m} | \bar{2} \rangle & \dots & \langle \bar{m} | \bar{m} \rangle & \langle \bar{m} | \\ \langle \bar{1} | & \langle \bar{2} | & \dots & \langle \bar{m} | & 0 \end{pmatrix}. \quad (16)$$

In Eqs. (15) and (16),  $\bar{m}$  represents the upper index for the Hermite Gaussian auxiliary functions. The Lagrange multiplier of the constraint (12) is denoted by  $\lambda$  in Eq. (14). In the following we will call  $\mathbf{J}$  the Coulomb vector and  $\mathbf{G}$  the auxiliary function Coulomb matrix. This matrix has the dimension  $\bar{n} = \bar{m} + 1$  according to the inclusion of the normalization constraint (12) in (14). It is build from the corresponding auxiliary function Coulomb matrix without constraint  $\mathbf{\Gamma}$  and the Hermite Gaussian integrals appearing in Eq. (12). The  $\mathbf{G}^{-1}$  matrix can be calculated from the inverse auxiliary function Coulomb matrix without constraint,  $\mathbf{\Gamma}^{-1}$ , by the Frobenius method.<sup>24</sup>

From the SCF energy expression (10) the Kohn-Sham matrix elements are obtained by differentiation with respect to the density matrix elements:

$$K_{\sigma\tau} = \frac{\partial E_{SCF}}{\partial P_{\sigma\tau}} = H_{\sigma\tau} + \sum_k^{\bar{m}} \langle \sigma\tau | \bar{k} \rangle x_k^- + \frac{\partial E_{xc}[\tilde{\rho}]}{\partial P_{\sigma\tau}}. \quad (17)$$

For the derivative of the exchange-correlation energy, restricting ourselves to local functionals for the clarity of the presentation, follows:

$$\frac{\partial E_{xc}[\tilde{\rho}]}{\partial P_{\sigma\tau}} = \int \frac{\delta E_{xc}[\tilde{\rho}]}{\delta \tilde{\rho}(\mathbf{r})} \frac{\partial \tilde{\rho}(\mathbf{r})}{\partial P_{\sigma\tau}} d\mathbf{r}. \quad (18)$$

The functional derivative defines the exchange-correlation potential calculated with the approximated density:

$$v_{xc}[\tilde{\rho}] = \frac{\delta E_{xc}[\tilde{\rho}]}{\delta \tilde{\rho}(\mathbf{r})}. \quad (19)$$

For the derivative of the approximated density with respect to the density matrix elements we find

$$\frac{\partial \tilde{\rho}(\mathbf{r})}{\partial P_{\sigma\tau}} = \sum_k \frac{\partial x_k^-}{\partial P_{\sigma\tau}} \bar{k}(\mathbf{r}). \quad (20)$$

From Eq. (14) follows:

$$\begin{aligned} x_k^- &= \sum_l^{\bar{n}} G_{kl}^{-1} J_l = \sum_l^{\bar{m}} G_{kl}^{-1} \sum_{\mu,\nu} P_{\mu\nu} \langle \mu\nu | \bar{l} \rangle \\ &+ G_{k\bar{n}}^{-1} \sum_{\mu,\nu} P_{\mu\nu} S_{\mu\nu}. \end{aligned} \quad (21)$$

Therefore, we obtain for the approximated density derivative (20) using the fact that the  $\mathbf{G}^{-1}$  matrix is symmetric:

$$\frac{\partial \tilde{\rho}(\mathbf{r})}{\partial P_{\sigma\tau}} = \sum_k^{\bar{m}} \left( \sum_l^{\bar{m}} \langle \sigma\tau | \bar{l} \rangle G_{lk}^{-1} + S_{\sigma\tau} G_{\bar{n}k}^{-1} \right) \bar{k}(\mathbf{r}). \quad (22)$$

Inserting the above expression (22) and the definition for the approximated exchange-correlation potential (19) into (18) gives the following explicit formula for the exchange-correlation energy derivative:

$$\begin{aligned} \frac{\partial E_{xc}[\tilde{\rho}]}{\partial P_{\sigma\tau}} &= \sum_l^{\bar{m}} \langle \sigma\tau | \bar{l} \rangle \sum_k^{\bar{m}} G_{lk}^{-1} \langle \bar{k} | v_{xc} \rangle \\ &+ S_{\sigma\tau} \sum_k^{\bar{m}} G_{\bar{n}k}^{-1} \langle \bar{k} | v_{xc} \rangle. \end{aligned} \quad (23)$$

With the introduction of the exchange-correlation fitting coefficients  $z_l^-$  defined as

$$z_l^- = \sum_k^{\bar{m}} G_{lk}^{-1} \langle \bar{k} | v_{xc} \rangle, \quad (24)$$

follows for the Kohn-Sham matrix elements:

$$K_{\sigma\tau} = H_{\sigma\tau} + S_{\sigma\tau} z_{\bar{n}}^- + \sum_k^{\bar{m}} \langle \sigma\tau | \bar{k} \rangle (x_k^- + z_k^-). \quad (25)$$

The  $z_l^-$  coefficients have to be calculated from the numerical integrals  $\langle \bar{k} | v_{xc} \rangle$ . They are spin-polarized coefficients. Because the explicit derivative of the approximated density with respect to the density matrix elements is calculated the SCF procedure is variational. For the implementation it is important to note that the fitting coefficients defined by Eq. (14) have to be used directly for the evaluation of the exchange-correlation potential in order to keep the calculation variational. Any manipulation of these coefficients, e.g., the mixing with previous coefficients, destroys the variational nature of the described approach. Of course, the coefficient mixing can be still used for the Coulombic terms in the SCF energy expression.

A technical problem may arise from an ill-conditioned  $\mathbf{\Gamma}$  matrix. If this problem encounters a singular value decomposition<sup>25</sup> for the inversion of  $\mathbf{\Gamma}$  is applied. In order to ensure a numerically stable SCF convergence the fitting of the approximated density has to be converged too. Therefore, we have introduced in deMon additionally to the energy convergence criterion a convergence criterion based on the following quantity:

$$\Delta = \sum_k^m \left[ \sum_l^m (x_l^{new} - x_l^{old}) \langle l | k \rangle \right]^2. \quad (26)$$

Here  $x_l^{new}$  and  $x_l^{old}$  denote expansion coefficients of the approximated density of two successive SCF iterations calculated according to formula (14). With SCF energy and approximated density (26) convergence thresholds of  $10^{-5}$ – $10^{-6}$  stable energies, energy gradients, and second derivatives can be obtained with the above described approximation.

### III. GRADIENTS

Based on the SCF energy expression (10) we find for the SCF energy gradients:

$$E_{SCF}^x = \sum_{\mu,\nu} P_{\mu\nu} \left( H_{\mu\nu}^x + \sum_{\bar{k}} \langle \mu\nu || \bar{k} \rangle^x x_{\bar{k}}^- \right) + \sum_{\mu,\nu} P_{\mu\nu}^x \left( H_{\mu\nu} + \sum_{\bar{k}} \langle \mu\nu || \bar{k} \rangle x_{\bar{k}}^- \right) - \frac{1}{2} \sum_{\bar{k},\bar{l}} x_{\bar{k}}^- x_{\bar{l}}^- \langle \bar{k} || \bar{l} \rangle^x + E_{xc}^x[\tilde{\rho}]. \quad (27)$$

Here the superscript  $x$  denotes differentiation with respect to a nuclear coordinate. The terms involving derivatives of the fitting coefficients vanish for a converged SCF solution due to Eq. (11). For the derivative of the exchange-correlation energy we find

$$E_{xc}^x[\tilde{\rho}] = \int \frac{\delta E_{xc}[\tilde{\rho}]}{\delta \tilde{\rho}(\mathbf{r})} \tilde{\rho}^x(\mathbf{r}) d\mathbf{r}. \quad (28)$$

The derivative of the approximated density with respect to a nuclear coordinate is given as

$$\tilde{\rho}^x(\mathbf{r}) = \sum_{\bar{k}} x_{\bar{k}}^- \bar{k}^x(\mathbf{r}) + x_{\bar{k}}^- \bar{k}^x(\mathbf{r}). \quad (29)$$

The derivatives of the fitting coefficients are obtained from the corresponding derivatives of equation system (14). Using the explicit form of the auxiliary function Coulomb matrix  $\mathbf{G}$ , (16), it follows:

$$\sum_{\bar{k}} \langle \bar{l} || \bar{k} \rangle^x x_{\bar{k}}^- + \sum_{\bar{k}} \langle \bar{l} || \bar{k} \rangle x_{\bar{k}}^- + \langle \bar{l} \rangle^x \lambda + \langle \bar{l} \rangle \lambda^x = J_{\bar{l}}^x \quad \forall \quad \bar{l} \leq \bar{m}, \quad (30)$$

$$\sum_{\bar{k}} \langle \bar{k} \rangle^x x_{\bar{k}}^- + \sum_{\bar{k}} \langle \bar{k} \rangle x_{\bar{k}}^- = \sum_{\mu,\nu} P_{\mu\nu}^x S_{\mu\nu} + \sum_{\mu,\nu} P_{\mu\nu} S_{\mu\nu}^x.$$

Because the Hermite Gaussian integral derivatives  $\langle \bar{k} \rangle^x$  vanish the following equation system is obtained:

$$\begin{pmatrix} \mathbf{x}^x \\ \lambda^x \end{pmatrix} = \mathbf{G}^{-1} \begin{pmatrix} \mathbf{J}^x - \mathbf{I}^x \mathbf{x} \\ \sum_{\mu,\nu} P_{\mu\nu}^x S_{\mu\nu} + \sum_{\mu,\nu} P_{\mu\nu} S_{\mu\nu}^x \end{pmatrix}, \quad (31)$$

with

$$x_{\bar{k}}^x = \sum_{\bar{l}} G_{\bar{k}\bar{l}}^{-1} \left( J_{\bar{l}}^x - \sum_{\bar{p}} \langle \bar{l} || \bar{p} \rangle^x x_{\bar{p}}^- \right) + G_{\bar{k}\bar{n}}^{-1} \left( \sum_{\mu,\nu} P_{\mu\nu}^x S_{\mu\nu} + \sum_{\mu,\nu} P_{\mu\nu} S_{\mu\nu}^x \right) \quad (32)$$

and

$$J_{\bar{l}}^x = \sum_{\mu,\nu} P_{\mu\nu}^x \langle \mu\nu || \bar{l} \rangle + \sum_{\mu,\nu} P_{\mu\nu} \langle \mu\nu || \bar{l} \rangle^x \quad (33)$$

follows further for the exchange-correlation energy derivative:

$$E_{xc}^x[\tilde{\rho}] = \sum_{\mu,\nu} P_{\mu\nu}^x \sum_{\bar{l}} \langle \mu\nu || \bar{l} \rangle^x z_{\bar{l}}^- + \sum_{\mu,\nu} P_{\mu\nu}^x S_{\mu\nu} z_{\bar{n}}^- + \sum_{\mu,\nu} P_{\mu\nu} \sum_{\bar{l}} \langle \mu\nu || \bar{l} \rangle^x z_{\bar{l}}^- + \sum_{\mu,\nu} P_{\mu\nu} S_{\mu\nu}^x z_{\bar{n}}^- - \sum_{\bar{k},\bar{l}} x_{\bar{k}}^- z_{\bar{l}}^- \langle \bar{k} || \bar{l} \rangle^x + \sum_{\bar{k}} x_{\bar{k}}^- \langle \bar{k}^x | v_{xc} \rangle. \quad (34)$$

Inserting the above expression for the exchange-correlation energy derivative into Eq. (27) gives

$$E_{SCF}^x = \sum_{\mu,\nu} P_{\mu\nu} \left( H_{\mu\nu}^x + S_{\mu\nu}^x z_{\bar{n}}^- + \sum_{\bar{k}} \langle \mu\nu || \bar{k} \rangle^x (x_{\bar{k}}^- + z_{\bar{k}}^-) \right) + \sum_{\mu,\nu} P_{\mu\nu}^x \left( H_{\mu\nu} + S_{\mu\nu} z_{\bar{n}}^- + \sum_{\bar{k}} \langle \mu\nu || \bar{k} \rangle (x_{\bar{k}}^- + z_{\bar{k}}^-) \right) - \sum_{\bar{k},\bar{l}} x_{\bar{k}}^- \left( z_{\bar{l}}^- + \frac{1}{2} x_{\bar{l}}^- \right) \langle \bar{k} || \bar{l} \rangle^x + \sum_{\bar{k}} x_{\bar{k}}^- \langle \bar{k}^x | v_{xc} \rangle. \quad (35)$$

The bracket of the second term in Eq. (35) represents a Kohn-Sham matrix element as defined in Eq. (25). Therefore, the Pulay relation<sup>26</sup> can be applied in order to eliminate the explicit derivatives of density matrix elements. With the modified energy weighted density matrix,

$$W_{\mu\nu} = \sum_i^{occ} (\varepsilon_i + z_{\bar{n}}^-) c_{\mu i} c_{\nu i}, \quad (36)$$

follows as final expression for the SCF energy gradient:

$$E_{SCF}^x = \sum_{\mu,\nu} P_{\mu\nu} \left( H_{\mu\nu}^x + \sum_{\bar{k}} \langle \mu\nu || \bar{k} \rangle^x (x_{\bar{k}}^- + z_{\bar{k}}^-) \right) - \sum_{\mu,\nu} W_{\mu\nu} S_{\mu\nu}^x - \sum_{\bar{k},\bar{l}} x_{\bar{k}}^- \left( z_{\bar{l}}^- + \frac{1}{2} x_{\bar{l}}^- \right) \langle \bar{k} || \bar{l} \rangle^x + \sum_{\bar{k}} x_{\bar{k}}^- \langle \bar{k}^x | v_{xc} \rangle. \quad (37)$$

### IV. COMPUTATIONAL METHODOLOGY

All calculations were performed with deMon<sup>22</sup> using the DZVP basis<sup>27</sup> and A2 or GEN-A2\* auxiliary function sets. The A2 auxiliary function set contains  $s$ ,  $p$ , and  $d$  auxiliary functions and has been optimized for the DZVP basis. The GEN-A2\* auxiliary function set possesses a similar structure as the A2 set but includes also  $f$  and  $g$  auxiliary functions. For the validation, the local Dirac exchange<sup>28</sup> in combination with the correlation functional proposed by Vosko, Wilk, and Nussair (VWN) (Ref. 29) as well as the gradient corrected exchange functional from Becke<sup>30</sup> in combination with the correlation functional from Lee, Yang, and Parr<sup>31,32</sup> (BLYP) have been used. For the numerical integration the standard adaptive grid (MEDIUM) from deMon was employed.<sup>33</sup> All geometry optimizations were performed in internal redundant coordinates without constraints.<sup>34</sup>

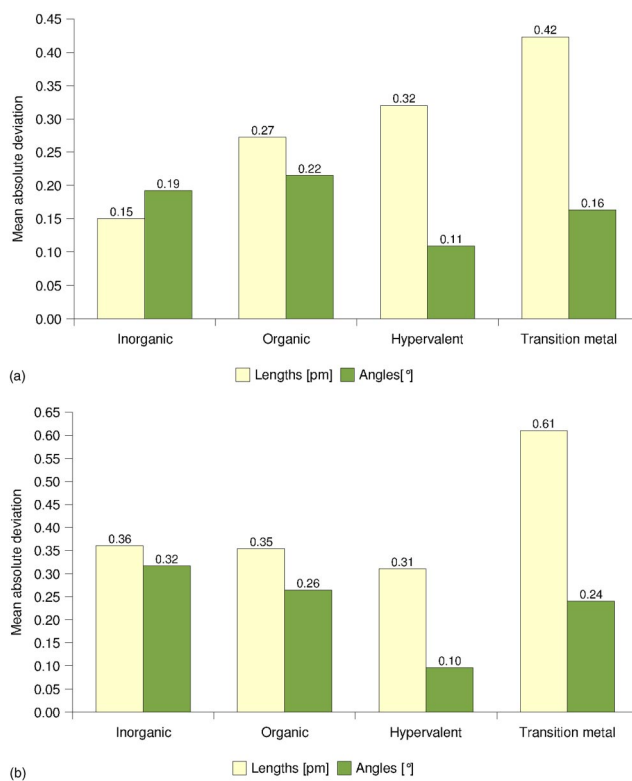


FIG. 1. Mean absolute deviations of optimized bond lengths (light bars) and bond angles (dark bars) using the approximated density for the calculation of the exchange-correlation potential. The top (a) refers to VWN and the bottom (b) to BLYP calculations using the A2 auxiliary function set.

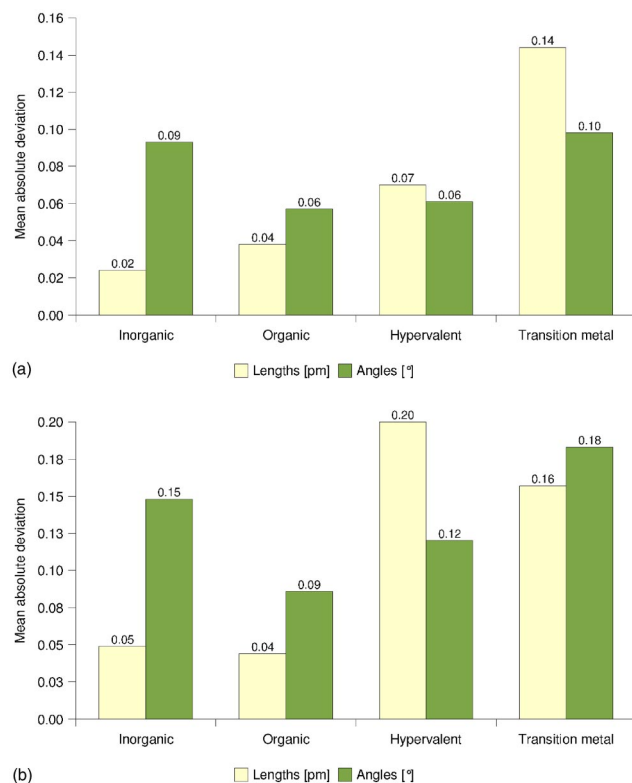


FIG. 2. Mean absolute deviations of optimized bond lengths (light bars) and bond angles (dark bars) using the approximated density for the calculation of the exchange-correlation potential. The top (a) refers to VWN and the bottom (b) to BLYP calculations using the GEN-A2\* auxiliary function set.



## V. VALIDATION AND PERFORMANCE

The mean absolute deviations of the optimized structure parameters employing the auxiliary function density for the calculation of the exchange-correlation potential are depicted in Figs. 1 and 2. In the reference calculations the orbital density is used for the calculation of the exchange-correlation energy and potential. The variational fitting of the Coulomb potential is used in both calculations. The test systems consist of 27 inorganic molecules (labeled Inorganic), 36 organic molecules (labeled Organic), 13 hypervalent molecules (labeled Hypervalent), and 71 transition metal systems (labeled Transition metal). All structure parameters are explicitly listed and compared to experiment in the supplementary material<sup>35</sup> of this article. The light bars represent the mean absolute deviation of the bond lengths and the dark bars the ones of the bond angles. Figure 1 shows the results obtained with the A2 auxiliary function set. The top (a) of the figure refers to the VWN calculations and the bottom (b) to the BLYP calculations.

Figure 1(a) shows that the mean absolute deviations for the VWN functional are smaller than 0.5 pm and 0.3°. The largest bond length deviations are found in the transition metal systems. The maximum deviation is 2.8 pm in these systems. The maximum bond length deviations for the other test sets are 1.0 pm (Inorganic), 1.1 pm (Organic), and 0.8 pm (Hypervalent). The maximum deviation in bond angles is smaller than 1.5° for all systems. For the BLYP functional slightly larger deviations are observed as Fig. 1(b) shows. Again the largest deviations are found for the transition metal systems. The maximum bond length deviation increases to 3.4 pm for the vanadium cyclopentadienyl bonds in  $V(C_5H_5)(CO)_4$ . The maximum bond length deviations for the other test sets are 1.8 pm (Inorganic), 1.1 pm (Organic), and 0.9 pm (Hypervalent). The maximum deviation in bond angles is again smaller than 1.5° for all systems.

In Fig. 2 the corresponding data for the GEN-A2\* auxiliary function set are depicted. Different to the A2 set the GEN-A2\* set also includes *f* and *g* functions. As a result a considerable reduction in the mean absolute deviations of the bond length are observed. The maximum deviation reduces to 2.0 pm for both functionals. For the local functional (Figure 2a) mean absolute deviations of less than 0.1 pm and maximum bond length deviations of less than 0.5 pm are found for the Inorganic, Organic, and Hypervalent test sets. These deviations are within the numerical accuracy of the method. For all test sets the maximum bond angle deviations are less than 1°. In Fig. 2(b) the corresponding absolute mean deviations for the BLYP functional are depicted. Again they are considerably smaller than for the A2 auxiliary function set. The maximum deviations are 0.3 pm (Inorganic), 0.8 pm (Organic), 1.1 pm (Hypervalent), and 2.0 pm (Transition metal) for the test sets.

From the above comparison we can conclude that the exchange-correlation potential calculation with the approximated density is well suited for the structure optimization. Excellent agreements, within the numerical accuracy of the method, are obtained for inorganic, organic, and hypervalent systems using the GEN-A2\* auxiliary function set. For the same systems the agreement is good with the A2 auxiliary

TABLE I. Atomization energies [kcal/mol] of selected dimers. The entries AUXIS and BASIS refer to the auxiliary function and orbital density used for the calculation of the exchange-correlation potential, respectively. The A2 and GEN-A2\* auxiliary function sets were used in combination with the BLYP functional. The experimental geometry was employed for all systems.

Molecule	A2		GEN-A2*	
	AUXIS	BASIS	AUXIS	BASIS
LiH	62.2	59.1	58.6	58.8
Li <sub>2</sub>	19.4	20.4	20.1	20.4
HF	142.6	139.2	139.0	138.5
LiF	135.7	137.3	138.3	137.3
NaH	47.9	46.3	45.5	46.1
N <sub>2</sub>	228.4	227.7	227.0	227.4
CO	252.4	253.0	253.1	252.7
F <sub>2</sub>	49.7	48.6	48.0	47.6
HCl	108.9	104.9	102.7	102.9
NaF	108.2	111.0	111.7	111.0
LiCl	105.0	107.0	107.1	107.0
PN	150.4	149.3	149.3	149.1
Na <sub>2</sub>	13.7	15.3	14.7	15.3
CS	165.6	166.2	165.8	166.0
CrH	60.5	59.1	56.5	57.5
MnH	44.3	40.6	39.7	39.4
ClF	61.2	61.2	60.8	60.2
CoH	95.4	92.5	90.2	90.1
NaCl	86.6	89.4	90.3	89.5
CuH	71.4	68.7	66.4	67.6
P <sub>2</sub>	115.3	114.1	113.9	113.9
MnO	120.3	122.5	121.0	121.9
FeO	132.8	133.7	135.2	134.3
Cl <sub>2</sub>	50.8	49.8	48.4	48.3
CuO	70.3	71.8	71.5	71.5
CuF	93.0	95.4	97.6	95.6
FeCl	81.2	82.1	82.2	82.2
CuCl	76.9	77.5	76.3	77.1
Cu <sub>2</sub>	48.0	48.0	49.4	49.4

function set. For the transition metal systems we observe larger maximum deviations in the range of 2–3 pm depending on the used functional and auxiliary function set. Nevertheless, these deviations are much smaller than the ones arising from the change of the functional.

In Table I the uncorrected atomization energies (BLYP) of selected dimers are listed. No correction for the zero point energy or basis set superposition error is employed. Thus, the differences in Table I are directly reflecting the errors due to the calculation of the exchange-correlation energy with the approximated density. For the calculation the experimental geometries (see the supplementary material) were employed. The values in the AUXIS columns refer to the calculation of the exchange-correlation energy with the auxiliary function density. The values in the BASIS columns refer to the calculation of the exchange-correlation energy with the orbital density and represent the reference data. All energies are given in kcal/mol.

For the A2 auxiliary function set a maximum error of 4 kcal/mol is found for the HCl molecule. The average error is under 2 kcal/mol. This accuracy is sufficient for most qualitative studies. Including *f* and *g* functions into the auxiliary function set, as in the GEN-A2\* set, reduces the average error to 0.5 kcal/mol. This error is in the range of the accuracy of the method and, therefore, acceptable even for quan-

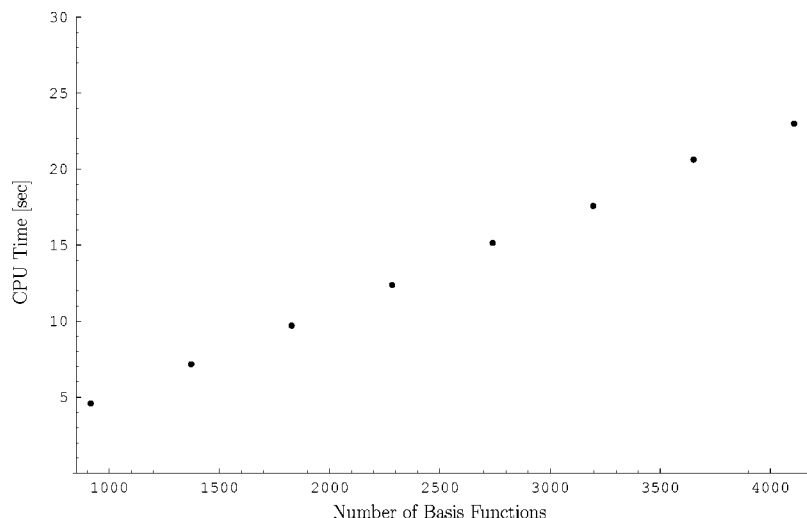


FIG. 3. CPU timings (SGI R14000, 500 MHz) for the numerical integration of the exchange-correlation potential for the alkenes  $C_{48}H_{98}$ ,  $C_{72}H_{146}$ ,  $C_{96}H_{194}$ ,  $C_{120}H_{242}$ ,  $C_{144}H_{290}$ ,  $C_{168}H_{338}$ ,  $C_{192}H_{386}$ , and  $C_{216}H_{434}$  using the approximated density.

titative studies. The maximum error for the GEN-A2\* set is 2 kcal/mol.

The timings for the numerical integration of the exchange-correlation potential for a series of alkenes are depicted in Fig. 3. The calculations were performed on a SGI R14000 (500 MHz) node. The DZVP basis and A2 auxiliary function set was used. For the calculation of the VWN functional the approximated density was employed. As Fig. 3 shows linear scaling is achieved. For the largest system,  $C_{216}H_{434}$  with around 4000 basis functions, the numerical integration of the exchange-correlation potential requires less than 25 sec. This clearly demonstrates the efficiency of the described approximation.

## VI. CONCLUSION

In this paper we have presented the basic working equations for the use of the auxiliary function density from the variational fitting of the Coulomb potential for the calculation of the exchange-correlation potential. It was shown that the resulting energy expression is variational and that reliable analytic gradients can be obtained. The approximation converges to the reference, which is the calculation of the exchange-correlation potential with the orbital density, by increasing the auxiliary function set. For accurate energy calculations auxiliary function sets with  $f$  and  $g$  functions are recommended. With these auxiliary function sets, like the here used GEN-A2\*, an average energy accuracy of around 0.5 kcal/mol can be obtained. For structure optimizations the A2 auxiliary function set, which contains only  $s$ ,  $p$ , and  $d$  functions, is sufficient for most applications.

With the above described approximation the CPU time for the numerical integration, prior a bottleneck in large scale calculations, becomes negligible. In combination with the recently described implementation of the three-center electron repulsion integral calculation<sup>11</sup> the construction of the Kohn-Sham matrix in LCGTO-DFT methods scales linear. Thus, the bottleneck of the calculation is shifted to the linear algebra operations, mainly the diagonalization. Especially if a singular value decomposition of the auxiliary function Coulomb matrix is necessary. Nevertheless, the current implementation in deMon allows routine calculations of sys-

tems with up to 6000 basis functions and has been already successfully applied to systems with more than 11 000 basis functions.

## ACKNOWLEDGMENTS

This work was financially supported by the CONACyT Projects No. G34037-E and 40379-F. J.U.R. and J.M.C. gratefully acknowledge CONACyT Ph.D. fellowships (Grants No. 154871 and 180545).

- <sup>1</sup>S. Obara and A. Saika, J. Chem. Phys. **84**, 3963 (1986).
- <sup>2</sup>M. Head-Gordon and J. A. Pople, J. Chem. Phys. **89**, 5777 (1988).
- <sup>3</sup>B. G. Johnson, P. M. W. Gill, J. A. Pople, and D. J. Fox, Chem. Phys. Lett. **206**, 239 (1993).
- <sup>4</sup>B. I. Dunlap, Int. J. Quantum Chem. **81**, 373 (2001).
- <sup>5</sup>M. Dupuis and A. Marquez, J. Chem. Phys. **114**, 2067 (2001).
- <sup>6</sup>B. I. Dunlap, J. W. D. Connolly, and J.R. Sabin, J. Chem. Phys. **71**, 4993 (1979).
- <sup>7</sup>J. W. Mintmire and B. I. Dunlap, Phys. Rev. A **25**, 88 (1982).
- <sup>8</sup>A. St-Amant and D. R. Salahub, Chem. Phys. Lett. **169**, 387 (1990).
- <sup>9</sup>O. Vahtras, J. Almlöf, and M.W. Feyereisen, Chem. Phys. Lett. **213**, 514 (1993).
- <sup>10</sup>K. Eichkorn, O. Treutler, H. Öhm, M. Häser, and R. Ahlrichs, Chem. Phys. Lett. **240**, 283 (1995).
- <sup>11</sup>A. M. Köster, J. Chem. Phys. **118**, 9943 (2003).
- <sup>12</sup>A. M. Köster, A. Goursot, and D. R. Salahub, in *Comprehensive Coordination Chemistry-II: From Biology to Nanotechnology*, edited by J. McCleverty, T. J. Meyer, and B. Lever (Elsevier, Amsterdam, 2003), Vol. 1.
- <sup>13</sup>E. J. Baerends, D. E. Ellis, and P. Ros, Chem. Phys. **2**, 41 (1973).
- <sup>14</sup>H. Sambe and R. H. Felton, J. Chem. Phys. **62**, 1122 (1975).
- <sup>15</sup>M. E. Casida, C. Daul, A. Goursot *et al.*, DEMON-KS Version 3.4, deMon Software, Montréal, 1996.
- <sup>16</sup>J. Andzelm and E. Wimmer, J. Chem. Phys. **96**, 1280 (1992).
- <sup>17</sup>J. C. Boettger and S. B. Trickey, Phys. Rev. B **53**, 3007 (1996).
- <sup>18</sup>D. N. Laikov, Chem. Phys. Lett. **281**, 151 (1997).
- <sup>19</sup>A. M. Köster, Habilitation thesis, Universität Hannover, 1998.
- <sup>20</sup>S. B. Trickey (private communication).
- <sup>21</sup>V. R. Saunders, in *Methods in Computational Physics*, edited by G. H. F. Dierksen and S. Wilson (Reidel, Dordrecht, 1983).
- <sup>22</sup>A. M. Köster, R. Flores-Moreno, G. Geudtner, A. Goursot, T. Heine, J. U. Reveles, A. Vela, and D. R. Salahub, deMon, NRC, Canada, 2003.
- <sup>23</sup>A. M. Köster, P. Calaminici, Z. Gómez, and U. Reveles, in *Reviews of Modern Quantum Chemistry, A Celebration of the Contribution of Robert G. Parr*, edited by K. Sen (World Scientific, New Jersey, 2002).
- <sup>24</sup>F. R. Gantmacher, *Matrizentheorie* (Springer, Berlin, 1986).
- <sup>25</sup>W. H. Press, S. A. Teukolsky, W. T. Vetterling, and B. P. Flannery, *Numerical Recipes in FORTRAN*, 2nd ed. (Cambridge University Press, Cambridge, 1992).
- <sup>26</sup>P. Pulay, Mol. Phys. **17**, 197 (1969).



- <sup>27</sup>N. Godbout, D. R. Salahub, J. Andzelm, and E. Wimmer, *Can. J. Phys.* **70**, 560 (1992).
- <sup>28</sup>P. A. M. Dirac, *Proc. Cambridge Philos. Soc.* **26**, 376 (1930).
- <sup>29</sup>S. H. Vosko, L. Wilk, and M. Nusair, *Can. J. Phys.* **58**, 1200 (1980).
- <sup>30</sup>A. D. Becke, *Phys. Rev. A* **38**, 3098 (1988).
- <sup>31</sup>C. Lee, W. Yang, and R. G. Parr, *Phys. Rev. B* **37**, 785 (1988).
- <sup>32</sup>B. Miehlich, A. Savin, H. Stoll, and H. Preuss, *Chem. Phys. Lett.* **157**, 200 (1989).
- <sup>33</sup>A. M. Köster, R. Flores-Moreno, and J. U. Reveles, *J. Chem. Phys.* **121**, 681 (2004); M. Krack and A. M. Köster, *ibid.* **108**, 3226 (1998).
- <sup>34</sup>J. U. Reveles and A. M. Köster, *J. Comput. Chem.* **25**, 1109 (2004).
- <sup>35</sup>See EPAPS Document No. JCPSA6-121-311430 for optimized and experimental structure parameters of the test set molecules. A direct link to this document may be found in the online article's HTML reference section. The document may also be reached via the EPAPS homepage (<http://www.aip.org/pubservs/epaps.html>) or from <ftp.aip.org> in the directory /epaps/. See the EPAPS homepage for more information.